DOI: 10.1002/ejic.200501086

Highly Symmetrical Tetranuclear Cluster Complexes Supported by *p-tert*-Butylsulfonylcalix[4]arene as a Cluster-Forming Ligand

Takashi Kajiwara,*[a] Takanori Kobashi,[b] Reiko Shinagawa,[b] Tasuku Ito,[b] Shinya Takaishi,[a] Masahiro Yamashita,[a] and Nobuhiko Iki*[c]

Keywords: Cluster compounds / Calixarenes / Magnetic properties / Ligand exchange

Square-planar tetranuclear clusters $[M_4(\mathbf{L})(AcO)_4(\mu_4\text{-}OH)]^-$ (M = Mn^{II}, Co^{II}, and Ni^{II}) are synthesized using tetra-anionic *p-tert*-butylsulfonylcalix[4]arene ($\mathbf{L}^{4-}$) as a cluster-forming ligand. Three complexes are crystallographically isostructural, being crystallized in the triclinic crystal system with space group $P\bar{1}$. The calix[4]arene acts as a tetrakis *fac*-tridentate ligand through four phenoxo and four sulfonyl oxygen atoms to form square arrangement of four metal ions, which are further bridged by four chelating acetate ions and one hydroxo ion in a μ_4 manner to complete the hexacoordination of each metal center. Although the whole molecule of each complex is crystallographically independent, the molecule is highly symmetrical with a pseudo-four-fold axis lying on the μ_4-OH^- group. The tetranuclear clusters are stable enough to maintain the core structures even in highly dilute solution (≈10 μM), which was confirmed by mass spectroscopic study, however, bridging acetates were easily exchanged by other carboxylate chelates to form derivatives such as $[M_4(\mathbf{L})(BzO)_4(OH)]^-$. Metal–metal interactions were investigated by means of magnetic susceptibility, and it was revealed that both ferro- and antiferromagnetic interactions occur in the Ni^{II} complex depending on the bridging angles of Ni–O–Ni.

Introduction

Multinuclear transition-metal complexes and metal clusters have attracted much attention owing to the interesting properties and the functionalities that originate from direct and/or indirect metal–metal interactions. Recent developments of synthetic methods for metal-based assemblies have enabled construction of a variety of well-organized architectures such as helicates,[1] cages,[2] and grids,[3] and the resulting assemblies are also interesting in their possibility to be novel materials incorporating magnetic, electronic, or optical features. For example, some square-shaped [2 × 2] dot systems having reversible redox properties are considered to be candidates for quantum-dot cellular automated devices.[3d,4] Synthetic strategies to produce such metal assemblies often employ well-designed multinucleating ligand systems.[5,6] As we have demonstrated, the thiacalix[*n*]arene[6a,6b,6c,6d] and its oxidized derivatives sulfonyl- and sulfinylcalix[*n*]arenes[6e,6f,6g,6h] can act as novel metal-assembling and cluster-forming ligands. We reported in previous papers that the thiacalix[6]arene gives tetranuclear and pentanuclear cluster complexes[6c,6d] when treated with first-row transition-metal acetate involving coordination bonds with 6 phenoxo oxygen and 6 sulfur atoms. In the case of pentanuclear clusters, hexa-anionic thiacalix[6]arene in the pinched-cone conformation formed a pocket-like cavity surrounded by 12 donor atoms. The cavity had an appropriate size to include a metal-cluster core, and five metal ions with compositions of Ni_4M (M = Co, Mn, or Cu) and Co_5 were included to form the pyramidally shaped cluster cores. Sulfonylcalix[4]arene (part a in Figure 1, $H_4\mathbf{L}$) led to octalanthanide cluster complexes ("lanthanide wheels") when it was treated with $Ln(AcO)_3 \cdot nH_2O$, in which each $\mathbf{L}^{4-}$ coordinated to one lanthanide ion as a tetradentate ligand through four phenoxo oxygen atoms,[6e] as the lanthanide ions with large ionic radii were in agreement with the cyclic donor system of $\mathbf{L}^{4-}$ to be included. However, for smaller ions such as first-row transition metals, $\mathbf{L}^{4-}$ and $H_2\mathbf{L}^{2-}$ act as a *fac*-tridentate ligand through three adjoining donor atoms, that is, two phenoxo and one sulfonyl oxygen atoms.[6f,6g] In a conic $H_{4-n}\mathbf{L}^{n-}$, eight donor atoms (four phenoxo and four axial sulfonyl oxygen atoms shown in Figure 1, b) are arranged in a flat manner where four *fac*-tridentate sites (**A**–**D**) are formed, each consisting of three donor oxygens. In the zinc(II) complex, $[Zn(H_2\mathbf{L})(tacn)]$ (tacn denotes 1,4,7-triazacyclononane), the zinc(II) ion

[a] Department of Chemistry, Graduate School of Science, Tohoku University and CREST, Japan Science and Technology Agency (JST),
Aoba-ku, Sendai 980-8578, Japan
Fax: +81-22-795-6547
E-mail: kajiwara@agnus.chem.tohoku.ac.jp
[b] Department of Chemistry, Graduate School of Science, Tohoku University,
Aoba-ku, Sendai 980-8578, Japan
[c] Department of Biomolecular Engineering, Graduate School of Engineering, Tohoku University,
Aoba-ku, Sendai 980-8579, Japan
E-mail: iki@orgsynth.che.tohoku.ac.jp
Supporting information for this article is available on the WWW under http://www.eurjic.org or from the author.

smoothly slides on this oxo-surface from one tridentate site to the adjoining site,[6f] and this result indicates that the four tridentate sites **A**–**D** in $\mathbf{L}^{4-}$ are equivalent and each site can bind a metal ion in a similar manner. As a result, $\mathbf{L}^{4-}$ can act as a tetranucleating ligand to give highly symmetrical square-planar clusters. Herein we report syntheses and properties of tetranuclear cluster complexes $(Me_4N)[M_4(\mathbf{L})(AcO)_4(\mu_4\text{-}OH)]$ {M^{II} = Mn^{II} (Me_4N[**1**]), Co^{II} (Me_4N[**2**]), and Ni^{II} (Me_4N[**3**])}, which are constructed on the basis of the cluster-forming ability of $\mathbf{L}^{4-}$.

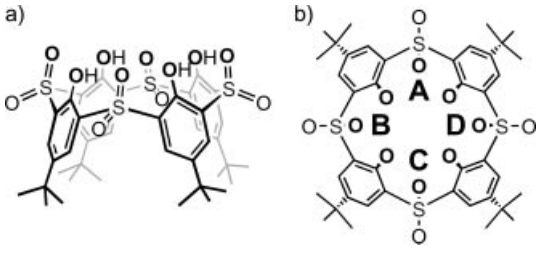

Figure 1. (a) Structure of *p*-(*tert*-butylsulfonyl)calix[4]arene ($H_4\mathbf{L}$). (b) Four equivalent coordination sites (**A**–**D**) of $\mathbf{L}^{4-}$.

Results and Discussion

Syntheses and Crystal Structures of Complexes

The reaction of $H_4\mathbf{L}$ and $Mn(AcO)_2{\cdot}4H_2O$ in a 1:5 ratio in $CHCl_3$/MeOH followed by crystallization from an EtOH/dimethylformamide (DMF) solution including Me_4NCl gave colorless crystals of Me_4N[**1**] in 36% yield. With a similar procedure, using $Co(AcO)_2{\cdot}4H_2O$ and $Ni(AcO)_2{\cdot}4H_2O$, Me_4N[**2**] and Me_4N[**3**] were also obtained in yields of 25 and 30%. In the formation of tetranuclear clusters, the acetate ions acted as a base to remove protons from $H_4\mathbf{L}$ to give $\mathbf{L}^{4-}$ and also from H_2O to give OH^-. To achieve the best yield, we found that the reaction ratio of the ligand and metal acetate must be 1:5 or larger.

Figure 2 shows the crystal structure of $[Mn_4(\mathbf{L})(AcO)_4(\mu_4\text{-}OH)]^-$ ($[\mathbf{1}]^-$). The complex crystallized in the triclinic crystal system and the four metal coordination sites are crystallographically independent of each other; however, the cluster is highly symmetrical and a pseudo-four-fold axis lies on the central μ_4-OH^- group (O13), and each metal ion is in a similar coordination environment. The conic $\mathbf{L}^{4-}$ supports the formation of the square Mn_4 cluster core. Four phenoxo (O3, O6, O9, and O12 in Figure 3) and four axial sulfonyl (O1, O4, O7, and O10) oxygen atoms form an almost flat surface with deviations from the ideal plane ranging from –0.132(3) to 0.220(3) Å, and $\mathbf{L}^{4-}$ acts as a tetrakis tridentate ligand through these eight oxygen atoms. Each Mn^{II} ion is ligated by one sulfonyl and two phenoxo oxygens in a *fac* manner similar to that found in $[Zn(H_2\mathbf{L})(tacn)]$, with distances of $Mn\text{–}O_{phenoxo}$ = 2.1550(18)–2.248(2) Å and $Mn\text{–}O_{sulfonyl}$ = 2.150(2)–2.1832(18) Å. Four AcO^- ions bridge adjoining Mn^{II} ion pairs [$Mn\text{–}O_{acetate}$ = 2.097(2)–2.132(2) Å], four Mn^{II} ions are further bridged by OH^- in an μ_4 manner [Mn–O13 = 2.2309(19)–2.3262(19) Å], and each Mn^{II} ion in $[\mathbf{1}]^-$ is in an octahedral coordination. Bridging hydroxide in an μ_4 manner is rather rare, and few complexes involving first-row transition-metal ions are reported in the Cambridge Crystallographic Data Base.[7] The most remarkable compounds in such a system are square-planar tetranuclear complexes constructed in the aperture of huge macrocyclic Schiff-base ligands reported by Edwards, Kruger, and McKee.[8] In our previous papers,[6d] we have demonstrated the formation of pyramidally arranged pentanuclear cluster complexes using thiacalix[6]arene, in which the basal four metal ions were also connected by OH^- in the same manner. In these complexes, the valence electrons from central oxygen are insufficient to make four M–O coordination bonds, which reflects the long bond lengths found not only in $[\mathbf{1}]^-$ but also in $[\mathbf{2}]^-$ and $[\mathbf{3}]^-$ mentioned below. Hence one can conclude that the μ_4-OH^- system is stable only in a cluster core with the support of huge macrocyclic ligands as a template. One crystal water molecule is bound to the μ_4-OH^- group through hydrogen bonding [O13···O22 = 2.747(6) Å], one DMF molecule is included in the cavity of conic $\mathbf{L}^{4-}$, and one tetramethylammonium ion is included in the lattice as a countercation. Me_4N[**2**] and Me_4N[**3**] are crystallographically isostructural to Me_4N[**1**], showing slight differences in

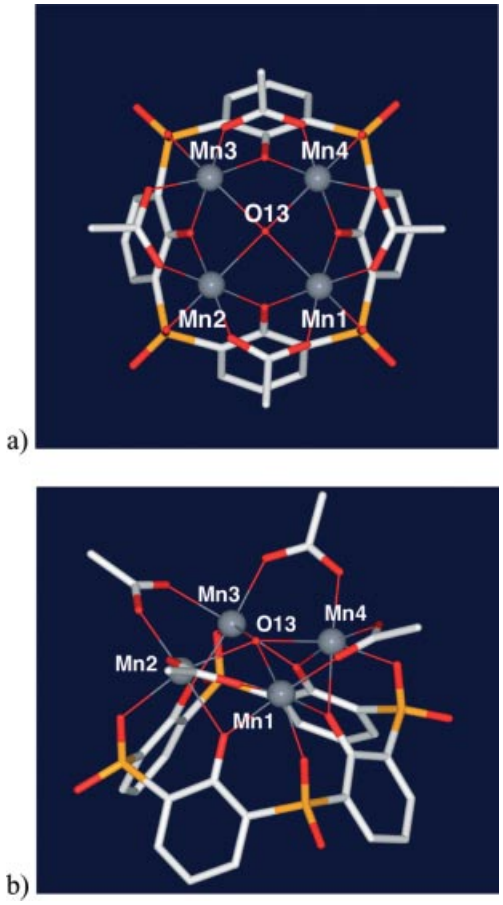

Figure 2. Crystal structure of $[\mathbf{1}]^-$. (a) Top view and (b) side view. *tert*-Butyl groups and hydrogen atoms are omitted. Each atom is depicted as follows: Mn^{II} gray, S orange, O red, and C white.

coordination distances. For $[\mathbf{2}]^-$, Co–$O_{phenoxo}$ distances were found in the range of 2.042(4)–2.117(4) Å, Co–$O_{sulfonyl}$ distances in 2.102(5)–2.121(4) Å, 2.013(5)–2.042(4) Å for Co–$O_{acetate}$, and Co–O13 was found to be 2.147(5)–2.290(5) Å. Coordination angles were found to fall in the range of 84.45(17)–92.32(17)°, and the Co^{II} ions are in a nearly ideal octahedral except for the slightly long bonding with the μ_4-OH^- group. For $[\mathbf{3}]^-$, nickel(II) ions are in a slightly elongated octahedral coordination with phenoxo and acetate oxygen atoms occupying equatorial positions [Ni–$O_{phenoxo}$ = 2.016(2)–2.072(2) and Ni–$O_{acetate}$ = 1.986(3)–2.005(3) Å] and sulfonyl and hydroxo oxygen atoms being at axial positions [Ni–$O_{sulfonyl}$ = 2.058(3)–2.079(2) and Ni–O13 = 2.142(3)–2.258(2) Å]. In $[\mathbf{3}]^-$, a residual electron peak with considerable density was found between the μ_4-OH^- group and a neighboring water molecule. This peak was assigned to a carbon atom and the reflection data were analyzed as a superposition of two molecules of $[Ni_4(\mathbf{L})(AcO)_4(\mu_4\text{-}OH)]^-$ ($[\mathbf{3}]^-$) and $[Ni_4(\mathbf{L})(AcO)_4(\mu_4\text{-}OMe)]^-$ ($[\mathbf{3b}]^-$) with 67% and 33% probabilities. The formation of μ_4-OMe bridged complex $[\mathbf{3b}]^-$ might be due to the higher acidity of Ni^{II} ion compared with Mn^{II} and Co^{II}. The presence of μ_4-OMe bridged species was also confirmed by mass spectroscopic studies (vide infra).

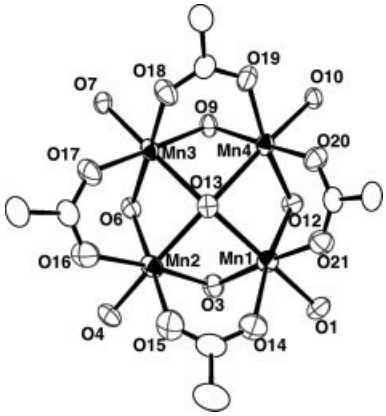

Figure 3. ORTEP diagram of tetranuclear manganese(II) core with thermal ellipsoids at 40% probability.

Ligand Exchange Reactions

The complexes maintain the tetranuclear cluster cores in a dilute MeCN solution, which was confirmed by ESI-mass spectroscopy. For $Me_4N[\mathbf{1}]$, intense parent peaks were observed at around *m*/*z* = 1317.0, which is related to $[Mn_4(\mathbf{L})(AcO)_4(OH)]^-$ (= $[\mathbf{1}]^-$) (Figure 4, a). Similar spectra were obtained for $[\mathbf{2}]^-$, with the main peaks positioned at around *m*/*z* = 1333.0 being related to $[Co_4(\mathbf{L})(AcO)_4(OH)]^-$ (= $[\mathbf{2}]^-$) (see Figure 1Sa in the Supporting Information), and for $[\mathbf{1}]^-$ and $[\mathbf{2}]^-$ minor species were observed at around *m*/*z* = 1292.9 and *m*/*z* = 1308.9 related to $[Mn_4(\mathbf{L})(AcO)_3(\mu_4\text{-}O)(H_2O)_2]^-$ (= $[\mathbf{1}]^-$ – AcOH + $2H_2O$) and $[Co_4(\mathbf{L})(AcO)_3(\mu_4\text{-}O)(H_2O)_2]^-$ (= $[\mathbf{2}]^-$ – AcOH + $2H_2O$), respectively. For $[\mathbf{3}]^-$, the main peaks at around *m*/*z* = 1306.9 and 1331.0 related to $[Ni_4(\mathbf{L})(AcO)_3(\mu_4\text{-}O)(H_2O)_2]^-$ (= $[\mathbf{3}]^-$ – AcOH + $2H_2O$) and $[Ni_4(\mathbf{L})(AcO)_4(\mu_4\text{-}OH)]^-$ (= $[\mathbf{3}]^-$), respectively, and a minor species involving μ_4-OMe $[Ni_4(\mathbf{L})(AcO)_4(\mu_4\text{-}OMe)]^-$ (= $[\mathbf{3b}]^-$) at around *m*/*z* = 1345.0 were observed (Figure 2Sa, Supporting Information). We assumed that the ligand exchange gave minor species such as $[M_4(\mathbf{L})(AcO)_3(\mu_4\text{-}O)(H_2O)_2]^-$, that is, μ_4-oxo-diaqua complexes. There are other possible formulas for these species including $[M_4(\mathbf{L})(AcO)_3(\mu_4\text{-}OH)(H_2O)(OH)]^-$, μ_4-hydroxo-aqua-hydroxo complexes, and this possibility was rejected by an absence of MS signals for corresponding $[Ni_4(\mathbf{L})(AcO)_3(\mu_4\text{-}OMe)(H_2O)(OH)]^-$ for $[\mathbf{3b}]^-$. The above results reveal that the tetranuclear cores in $[\mathbf{1}]^-$–$[\mathbf{3}]^-$ are stable enough to maintain their core structures even in a highly dilute coordinating solvent (≈10 μM), and moreover, formation of $[M_4(\mathbf{L})(AcO)_3(O)(H_2O)_2]^-$ species indicate that bridging acetate ions can be removed to realize a ligand exchange reaction to give some derivative complexes even in a mild condition. To confirm this, an exchange reaction of bridging acetate by benzoate was performed for all complexes. When $[\mathbf{1}]^-$ was treated with an excess of benzoic acid (1:5 molar ratio) in acetonitrile at ambient temperature, ligand exchange soon occurred to give a mixture of $[Mn_4(\mathbf{L})(AcO)_{4-n}(BzO)_n(OH)]^-$ (n = 2–4) and $[Mn_4(\mathbf{L})(AcO)_{3-m}(BzO)_m(O)(H_2O)_2]^-$ (m = 2–3), which was confirmed by FT-MS (Figure 4, b), and also by X-ray crystallography for $[Mn_4(\mathbf{L})(BzO)_4(OH)]^-$ (Figure 3S). Specific peaks were observed in Figure 4, b where $[Mn_4(\mathbf{L})(BzO)_4(OH)]^-$ was found to be a major component. To complete the exchange reaction, the mixed solution was evaporated once to dryness to remove AcOH, and the residue was again dissolved to the same solvent (Figure 4, c). The mass spectrum for this solution shows two main signals at around *m*/*z* = 1479.0 and 1565.0, being related to $[Mn_4(\mathbf{L})(BzO)_3(O)(H_2O)_2]^-$ and $[Mn_4(\mathbf{L})(BzO)_4(OH)]^-$, respectively, indicating that the acetate bridges were exchanged by benzoate almost quantitatively. The resulting $[Mn_4(\mathbf{L})(BzO)_4(OH)]^-$ was isolated as single crystals with the yield higher than 70%. Similar reactions for $[\mathbf{2}]^-$ and $[\mathbf{3}]^-$ also give the same result. For $[\mathbf{2}]^-$, the main signals at around *m*/*z* = 1495.0 and 1581.0 were observed for the reaction solution, which are related to $[Co_4(\mathbf{L})(BzO)_3(O)(H_2O)_2]^-$ and $[Co_4(\mathbf{L})(BzO)_4(OH)]^-$, respectively, and for $[\mathbf{3}]^-$ the main peaks at around *m*/*z* = 1493.0 and 1579.0 related to $[Ni_4(\mathbf{L})(BzO)_3(O)(H_2O)_2]^-$ and $[Ni_4(\mathbf{L})(BzO)_4(OH)]^-$ were found, indicating that $[Co_4(\mathbf{L})(BzO)_4(OH)]^-$ and $[Ni_4(\mathbf{L})(BzO)_4(OH)]^-$ should be the main products for both cases (Figure 1Sc and Figure 2Sc, respectively). For the case of $[\mathbf{3}]^-$, minor species involving μ_4-OMe formulated as $[Ni_4(\mathbf{L})(BzO)_4(OMe)]^-$ at around *m*/*z* = 1593.0 were observed in Figure 3Sc. The observed ratio between μ_4-OH species ($[Ni_4(\mathbf{L})(AcO)_3(O)(H_2O)_2]^-$ and $[Ni_4(\mathbf{L})(AcO)_4(OH)]^-$ for acetate-bridged complexes, and $[Ni_4(\mathbf{L})(BzO)_3(O)(H_2O)_2]^-$ and $[Ni_4(\mathbf{L})(BzO)_4(OH)]^-$ for benzoate-bridged complexes) and μ_4-OMe species ($[Ni_4(\mathbf{L})(AcO)_4(OMe)]^-$ and $[Ni_4(\mathbf{L})(BzO)_4(OMe)]^-$, respectively) were estimated to be similar for acetate-bridged species (64.6:35.4) and for benzoate-bridged species (64.9:35.1), indicating that the exchange of the central μ_4-OH group does not occur during

the exchange reaction of bridging carboxylates. This result suggests that core fragmentation does not occur during this reaction.

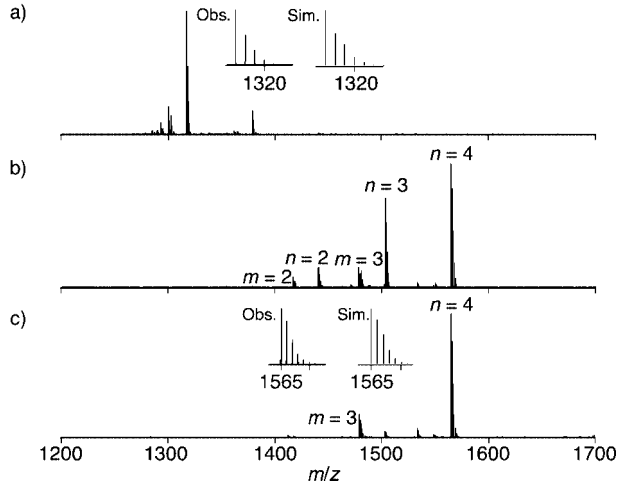

Figure 4. ESI-mass spectra of (a) complex Me_4N[**1**] in acetonitrile, (b) mixtures of benzoic acid and Me_4N[**1**] in a 5:1 ratio in acetonitrile, and (c) reaction products which were obtained by drying up the reaction solution of benzoic acid and Me_4N[**1**]. *n* and *m* denote the numbers of bridging benzoic groups in the species of $[M_4(\mathbf{L})(AcO)_{4-n}(BzO)_n(OH)]^-$ and $[M_4(\mathbf{L})(AcO)_{3-m}(BzO)_m(O)(H_2O)_2]^-$, respectively.

As the complexes maintain their cluster cores in the solution, electrochemical behaviors of these clusters in the same solution were preliminarily investigated by the cyclic voltammetry method at room temperature. No significant peak was observed in the range of –1.0 to +1.0 V versus Ag/Ag^+ for all three complexes (Figure 4S), indicating that the divalent tetranuclear complexes are rather stable under the experimental conditions.

Magnetic Behavior

To investigate the metal–metal interactions in square-shaped clusters, dc-magnetic susceptibilities were measured in the temperature range of 2–300 K. The $\chi_M T$ versus T plots for these complexes show continuous decreases of $\chi_M T$ values as the temperature is lowered (Figure 5, a). The $\chi_M T$ value at room temperature for Me_4N[**2**] is larger than the expected spin-only value for four isolated $S = 3/2$ spins, being due to the spin-orbit interactions, which is frequently observed for the Co^{II} ion in a slightly distorted octahedron,[9] and the magnitude of the interaction was hard to analyze. For Me_4N[**1**] and Me_4N[**3**], temperature dependences of the $\chi_M T$ values were analyzed on the basis of the Hamiltonian,[9]

$$\boldsymbol{H} = -2J_1\Sigma(\boldsymbol{S}_1\cdot\boldsymbol{S}_2 + \boldsymbol{S}_2\cdot\boldsymbol{S}_3 + \boldsymbol{S}_3\cdot\boldsymbol{S}_4 + \boldsymbol{S}_4\cdot\boldsymbol{S}_1) - 2J_2\Sigma(\boldsymbol{S}_1\cdot\boldsymbol{S}_3 + \boldsymbol{S}_2\cdot\boldsymbol{S}_4)$$

where J_1 denotes the interaction between adjoining metal ions and J_2 is for the diagonal metal ions (Figure 5, b). The best-fit parameters were obtained as $J_1 = -3.0\ cm^{-1}$ and $J_2 = -4.4\ cm^{-1}$ for Me_4N[**1**] and $J_1 = 24.9\ cm^{-1}$ and $J_2 = -43.9\ cm^{-1}$ for Me_4N[**3**]. For Ni^{II} ions, it is widely thought that the character of magnetic interactions clearly depends

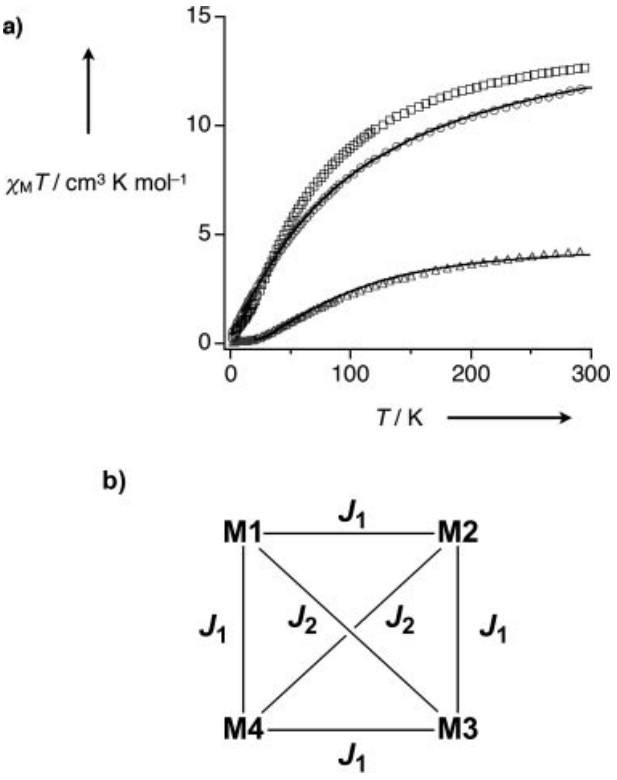

Figure 5. (a) Plots of $\chi_M T$ vs. T for Me_4N[**1**] (circle), Me_4N[**2**] (square), and Me_4N[**3**] (triangle). The solid lines correspond to the theoretical curves for which parameters are given in the text. (b) A schematic drawing of J_1 and J_2.

on the bridging angle.[10] As two spins are located on the e_g orbitals with dσ characters for Ni^{II}, a strict orbital orthogonality occurs and ferromagnetic interaction operates when the bridging angle is smaller than 100°, and a strong antiferromagnetic interaction occurs when the bridging angle reaches linearity. In Me_4N[**3**], because each adjoining Ni^{II} ion is bridged by two oxygen atoms involving one phenoxo and one μ_4-hydroxo oxygen atom with angles of 84.13(9)–93.18(10)°, a ferromagnetic interaction operates between two neighboring Ni^{II} ions with relatively strong magnitude. However, the diagonal Ni^{II} ions (two sets of Ni1/Ni3 and Ni2/Ni4) are bridged by the μ_4-OH^- group with angles of 144.88(12)° and 146.87(12)°, so an antiferromagnetic interaction occurs between nickel(II) ions in these two sets. In Me_4N[**1**], as the Mn^{II} ion has dσ and dπ spins, orbital overlap through bridging oxygen atoms occurs both in adjoining Mn^{II} sets and in diagonal Mn^{II} sets, and this causes antiferromagnetic interactions in both pathways.

Conclusion

In conclusion, a tetra-anionic sulfonylcalix[4]arene was used to construct three tetranuclear clusters having a highly symmetrical structure. The complexes are stable enough to maintain their structures in solution and moderate metal–metal interactions were estimated by magnetic susceptibility measurements. It is expected that $\mathbf{L}^{4-}$ generally acts as a tetranucleating ligand for other transition-metal ions, and

further studies for the development of a square-shaped tetranuclear system with reversible redox features are now in progress.

Experimental Section

Solvents and chemicals except for acetonitrile were purchased as reagent grade and used without further purification. Acetonitrile was distilled from calcium hydride immediately prior to use in the cyclic voltammetry measurements. ESI-MS experiments were performed using a Fourier Transform Ion Cyclotron Resonance (FTICR) mass spectrometer APEX III (Bruker). The reaction solution was diluted with acetonitrile, methanol, or acetonitrile/dichloromethane (1:1 v/v) to allow the mass spectroscopic measurement, which gave the same result. Variable-temperature magnetic susceptibility measurements were made using a SQUID magnetometer MPMS 5S (Quantum Design) at 1 T for Me_4N[**2**], and 0.25 T and 0.5 T field for Me_4N[**1**] and Me_4N[**3**], respectively. Diamagnetic correction for each sample was determined from Pascal's constants.

Synthesis of Me_4N[1] (Table 1): $Mn(AcO)_2{\cdot}4H_2O$ (12.3 mg, 0.05 mmol) and H_4**L** (8.5 mg, 0.01 mmol) were mixed and refluxed in MeOH/$CHCl_3$ (1:1, v/v, 10 mL) for an hour, and the solvents evaporated to dryness. The pale brown residue was dissolved into DMF (0.5 mL), added to Me_4NCl (2.2 mg, 0.02 mmol) in ethanol (2 mL), and then evaporated slowly. Colorless crystals of Me_4N[**1**]·3.5DMF·H_2O were formed in two weeks. Crystals were filtered and dried in vacuo. Yield, 5.2 mg, 36%. $C_{53.5}H_{74.5}Mn_4N_{1.5}O_{22.5}S_4$ (Me_4N[**1**]·0.5DMF·H_2O; 1446.69): calcd. C 44.42, H 5.19, N 1.45; found C 44.25, H 5.32, N 1.46.

Table 1. Selected bond lengths [Å] and angles [°] for Me_4N[**1**].

Mn1–O1	2.179(2)	Mn3–O6	2.1550(18)
Mn1–O3	2.213(2)	Mn3–O7	2.1832(18)
Mn1–O12	2.227(2)	Mn3–O9	2.233(2)
Mn1–O13	2.289(2)	Mn3–O13	2.3262(19)
Mn1–O14	2.115(2)	Mn3–O17	2.132(2)
Mn1–O21	2.100(2)	Mn3–O18	2.097(2)
Mn2–O3	2.240(2)	Mn4–O9	2.248(2)
Mn2–O4	2.150(2)	Mn4–O10	2.173(2)
Mn2–O6	2.2284(19)	Mn4–O12	2.2335(19)
Mn2–O13	2.2449(18)	Mn4–O13	2.2309(19)
Mn2–O15	2.122(2)	Mn4–O19	2.1108(19)
Mn2–O16	2.122(2)	Mn4–O20	2.111(2)
Mn1–O3–Mn2	89.17(6)	Mn2–O6–Mn3	90.24(8)
Mn1–O13–Mn2	87.16(6)	Mn2–O13–Mn3	85.60(7)
Mn1–O13–Mn3	150.37(7)	Mn2–O13–Mn4	153.41(7)
Mn1–O12–Mn4	88.62(7)	Mn3–O9–Mn4	88.49(6)
Mn1–O13–Mn4	87.16(7)	Mn3–O13–Mn4	86.61(7)

Synthesis of Me_4N[2] (Table 2): $Co(AcO)_2{\cdot}4H_2O$ (12.5 mg, 0.05 mmol) and H_4**L** (8.5 mg, 0.01 mmol) were mixed and refluxed in MeOH/$CHCl_3$ (1:1, v/v, 10 mL) for an hour, and the solvents evaporated to dryness. The pink residue was dissolved into DMF (0.5 mL), added to Me_4NCl (2.2 mg, 0.02 mmol) in ethanol (2 mL), and then evaporated slowly. Pink crystals of Me_4N[**2**]·2DMF·2H_2O·EtOH were formed in two weeks. Crystals were filtered and dried in vacuo. Yield, 4.3 mg, 30%. $C_{52}H_{71}Co_4NO_{22}S_4$ (Me_4N[**2**]·H_2O; 1426.13): calcd. C 43.80, H 5.02, N 0.98; found C 43.49, H 5.15, N 1.24.

Table 2. Selected bond lengths [Å] and angles [°] for Me_4N[**2**].

Co1–O1	2.117(5)	Co3–O6	2.042(4)
Co1–O3	2.100(4)	Co3–O7	2.121(4)
Co1–O12	2.096(5)	Co3–O9	2.100(4)
Co1–O13	2.228(5)	Co3–O13	2.290(5)
Co1–O14	2.014(5)	Co3–O17	2.029(5)
Co1–O21	2.020(5)	Co3–O18	2.013(5)
Co2–O3	2.106(5)	Co4–O9	2.117(4)
Co2–O4	2.102(5)	Co4–O10	2.120(5)
Co2–O6	2.110(4)	Co4–O12	2.108(5)
Co2–O13	2.165(5)	Co4–O13	2.147(5)
Co2–O15	2.042(4)	Co4–O19	2.028(5)
Co2–O16	2.034(5)	Co4–O20	2.024(5)
Co1–O3–Co2	90.88(17)	Co2–O6–Co3	92.32(17)
Co1–O13–Co2	86.04(18)	Co2–O13–Co3	84.45(17)
Co1–O13–Co3	146.9(2)	Co2–O13–Co4	149.3(3)
Co1–O12–Co4	91.26(19)	Co3–O9–Co4	91.21(16)
Co1–O13–Co4	86.75(19)	Co3–O13–Co4	85.48(17)

Synthesis of Me_4N[3] (Table 3): $Ni(AcO)_2{\cdot}4H_2O$ (12.4 mg, 0.05 mmol) and H_4**L** (8.5 mg, 0.01 mmol) were mixed and refluxed in MeOH/$CHCl_3$ (1:1, v/v, 10 mL) for an hour, and the solvents evaporated to dryness. The pale green residue was dissolved into DMF (0.5 mL), added to Me_4NCl (2.2 mg, 0.02 mmol) in ethanol (2 mL), and then evaporated slowly. Pale green crystals of Me_4N·0.67[**3**]·0.33[**3b**]·3.5DMF·0.67H_2O were formed in two weeks. Crystals were filtered and dried in vacuo. Yield 3.6 mg, 25%. $C_{52.33}H_{71}NNi_4O_{21.67}S_4$ (Me_4N·0.67[**3**]·0.33[**3b**]·0.67H_2O; 1423.85): calcd. C 44.14, H 5.03, N 0.98; found C 43.75, H 5.26, N 1.33.

Table 3. Selected bond lengths [Å] and angles [°] for Me_4N[**3**].

Ni1–O1	2.077(3)	Ni3–O6	2.016(2)
Ni1–O3	2.051(2)	Ni3–O7	2.079(2)
Ni1–O12	2.056(3)	Ni3–O9	2.066(2)
Ni1–O13	2.216(3)	Ni3–O13	2.258(2)
Ni1–O14	1.986(3)	Ni3–O17	2.003(3)
Ni1–O21	2.004(3)	Ni3–O18	1.986(3)
Ni2–O3	2.061(2)	Ni4–O9	2.072(2)
Ni2–O4	2.058(3)	Ni4–O10	2.071(3)
Ni2–O6	2.064(2)	Ni4–O12	2.068(3)
Ni2–O13	2.165(3)	Ni4–O13	2.142(3)
Ni2–O15	2.001(3)	Ni4–O19	1.999(3)
Ni2–O16	2.004(3)	Ni4–O20	2.005(3)
Ni1–O3–Ni2	92.29(10)	Ni2–O6–Ni3	93.18(10)
Ni1–O13–Ni2	85.20(9)	Ni2–O13–Ni3	84.13(9)
Ni1–O13–Ni3	144.88(12)	Ni2–O13–Ni4	146.87(12)
Ni1–O12–Ni4	91.97(10)	Ni3–O9–Ni4	92.08(10)
Ni1–O13–Ni4	85.77(9)	Ni3–O13–Ni4	85.17(9)

X-ray Crystallography: Data for all of the compounds were collected by a Bruker SMART APEX diffractometer employing graphite-monochromated Mo-K_α radiation (λ = 0.71073 Å) at low temperature (200–233 K). The data integration and reduction were undertaken with SAINT and XPREP.[11] An empirical correction determined with SADABS[12] was applied to all data. The structures were solved by the direct method using SHELXS-97[13] and refined using least-squares methods on F^2 with SHELXL-97.[13] Non-hydrogen atoms were modeled with anisotropic displacement parameters, and hydrogen atoms were placed by the differential Fourier syntheses and refined isotropically (Table 4).

CCDC-249858 to -249860 contain the supplementary crystallographic data for this paper. These data can be obtained free of charge from The Cambridge Crystallographic Data Centre via www.ccdc.cam.ac.uk/data_request/cif.

Table 4.Crystallographic data and structural refinement for Me_4N[**1**]–Me_4N[**3**].

	Me_4N[**1**]·3.5DMF·H_2O	Me_4N[**2**]·2DMF·$2H_2O$·EtOH	Me_4N·0.67[**3**]·0.33[**3b**]·3.5DMF·$0.67H_2O$
Empirical formula	$C_{62.5}H_{90}Mn_4N_{4.5}O_{25.5}S_4$	$C_{60}H_{93}Co_4N_3O_{26}S_4$	$C_{62.83}H_{95.5}N_{4.5}Ni_4O_{25.17}S_4$
Formula mass	1660.39	1636.33	1680.50
Crystal system	triclinic	triclinic	triclinic
Space group	$P\bar{1}$	$P\bar{1}$	$P\bar{1}$
a [Å]	14.158(11)	14.093(2)	14.0698(14)
b [Å]	14.469(12)	14.278(2)	14.2101(14)
c [Å]	18.983(15)	18.796(3)	18.8762(19)
α [°]	87.463(17)	87.765(5)	87.151(2)
β [°]	89.952(16)	89.435(5)	89.546(2)
γ [°]	86.414(16)	86.276(5)	86.462(2)
V [Å^3]	3877(5)	3771.3(11)	3762.1(6)
Z	2	2	2
F (000)	1729	1708	1764
T [K]	200(2)	183(2)	200(2)
$\rho_{calcd.}$ [g cm^{-3}]	1.422	1.441	1.484
Reflections collected	28627	30747	30925
Independent reflections	13600 [R_{int} = 0.0841]	13239 [R_{int} = 0.0924]	13231 [R_{int} = 0.0555]
μ [mm^{-1}]	0.820	1.051	1.175
R_1, wR_2 [$I > 2\sigma(I)$]	0.0628, 0.01361	0.0707, 0.1323	0.0417, 0.0904
R_1, wR_2 (all data)	0.1259, 0.1588	0.1601, 0.1544	0.0760, 0.0974
Gof (for F^2)	0.932	0.897	0.861

Supporting Information (for details see the footnote on the first page of this article): ESI-mass spectra of complexes Me_4N[**2**] and Me_4N[**3**], crystal structure of $[Mn(\mathbf{L})(BzO)_4(OH)]^-$, and cyclic voltammograms of Me_4N[**1**] to Me_4N[**3**] (Figures 1S–4S).

Acknowledgments

This work was supported by a Grant-in Aid for Scientific Research from the Ministry of Education, Culture, Sports, Science, and Technology, Japan.

[1] For example: C. Piguet, G. Bernardinelli, G. Hopfgartner, *Chem. Rev.* **1997**, *97*, 2005–2062.

[2] a) P. N. W. Baxter, J.-M. Lehn, G. Baum, D. Fenske, *Chem. Eur. J.* **1999**, *5*, 102–112; b) P. N. W. Baxter, J.-M. Lehn, B. O. Kneisel, G. Baum, D. Fenske, *Chem. Eur. J.* **1999**, *5*, 113–120; c) J. S. Fleming, K. L. V. Mann, C.-A. Carraz, E. Psillakis, J. C. Jeffery, J. A. McCleverty, M. D. Ward, *Angew. Chem. Int. Ed.* **1998**, *37*, 1279–1281; d) A. Kamiyama, T. Kajiwara, T. Ito, *Chem. Lett.* **2002**, 980–981.

[3] a) G. S. Hanan, D. Volkmer, U. S. Schubert, J.-M. Lehn, G. Baum, D. Fenske, *Angew. Chem. Int. Ed. Engl.* **1997**, *36*, 1842–1844; b) D. M. Bassani, J.-M. Lehn, K. Fromm, D. Fenske, *Angew. Chem. Int. Ed.* **1998**, *37*, 2364–2367; c) L. Zhao, Z. Xu, L. K. Thompson, S. L. Heath, D. O. Miller, M. Ohba, *Angew. Chem. Int. Ed.* **2000**, *39*, 3114–3117; d) L. H. Uppadine, J.-M. Lehn, *Angew. Chem. Int. Ed.* **2004**, *43*, 240–243.

[4] C. S. Lent, B. Isaksen, M. Lieberman, *J. Am. Chem. Soc.* **2003**, *125*, 1056–1063.

[5] For example: a) S. S. Tandon, L. K. Thompson, J. N. Bridson, C. Benelli, *Inorg. Chem.* **1995**, *34*, 5507–5515; b) B. F. Hoskins, R. Robson, P. Smith, *J. Chem. Soc., Chem. Commun.* **1990**, 488–489; c) H. C. Aspinall, J. Black, I. Dodd, M. M. Harding, S. J. Winkley, *J. Chem. Soc., Dalton Trans.* **1993**, 709–714; d) S. Brooker, V. McKee, W. B. Shepard, L. K. Pannell, *J. Chem. Soc., Dalton Trans.* **1987**, 2555–2562; e) S. Cromie, F. Launay, V. McKee, *Chem. Commun.* **2001**, 1918–1919; f) M. Yonemura, H. Okawa, M. Ohba, D. E. Fenton, L. K. Thompson, *Chem. Commun.* **2000**, 817–818.

[6] a) H. Akdas, E. Graf, M. W. Hosseini, A. De Cian, A. Bilyk, B. W. Skelton, G. A. Koutsantonis, I. Murray, J. M. Harrowfield, A. H. White, *Chem. Commun.* **2002**, 1042–1043; b) A. Bilyk, A. K. Hall, J. M. Harrowfield, M. W. Hosseini, B. W. Skelton, A. H. White, *Inorg. Chem.* **2001**, *40*, 672–686; c) T. Kajiwara, N. Kon, S. Yokozawa, T. Ito, N. Iki, S. Miyano, *J. Am. Chem. Soc.* **2002**, *124*, 11274–11275; d) T. Kajiwara, R. Shinagawa, T. Ito, N. Kon, N. Iki, S. Miyano, *Bull. Chem. Soc. Jpn.* **2003**, *76*, 2267–2275; e) T. Kajiwara, H. Wu, T. Ito, N. Iki, S. Miyano, *Angew. Chem. Int. Ed.* **2004**, *43*, 1832–1835; f) T. Kajiwara, S. Yokozawa, T. Ito, N. Iki, N. Morohashi, S. Miyano, *Angew. Chem. Int. Ed.* **2002**, *41*, 2076–2078; g) T. Kajiwara, S. Yokozawa, T. Ito, N. Iki, N. Morohashi, S. Miyano, *Chem. Lett.* **2001**, 6–7; h) N. Morohashi, N. Iki, S. Miyano, T. Kajiwara, T. Ito, *Chem. Lett.* **2001**, 66–67.

[7] Conquest, Software for searching the Cambridge Structural Database and visualizing crystal structures: I. J. Bruno, J. C. Cole, P. R. Edgington, M. Kessler, C. F. Macrae, P. McCabe, J. Pearson, R. Taylor, *Acta Crystallogr., Sect. B* **2002**, *58*, 389–397.

[8] a) A. J. Edwards, B. F. Hoskins, E. H. Kachab, A. Markiewicz, K. S. Murray, R. Robson, *Inorg. Chem.* **1992**, *31*, 3585–3591; b) P. E. Kruger, V. McKee, *Chem. Commun.* **1997**, 1341–1342; c) J. McKee, V. McKee, T. Metcalfe, S. S. Tandon, J. Wikaira, *Inorg. Chim. Acta* **2000**, *297*, 220–230.

[9] O. Kahn, *Molecular Magnetism*, VCH, Weinheim, **1993**.

[10] M. A. Halcrow, J.-S. Sun, J. C. Huffman, G. Christou, *Inorg. Chem.* **1995**, *34*, 4167–4177.

[11] SMART, SAINT and XPREP, Area detector control and data integration and reduction software, Bruker Analytical X-ray Instruments Inc., Madison, WI, **1995**.

[12] G. M. Sheldrick, SADABS, Empirical absorption correction program for area detector data, University of Göttingen, Germany, **1996**.

[13] G. M. Sheldrick, SHELX97, Programs for Crystal Structure Analysis, University of Göttingen, Germany, **1998**.

Received: December 5, 2005
Published Online: March 6, 2006

